

# The role of doping $\text{Cr}_2\text{O}_3$ on the structural modification of oxyfluoroborate glasses using X-Ray and Raman Spectroscopy

A. ABOU SHAMA\*, M. BAKR MOHAMED, K. EL-SAYED

*XRD Unit, Physics Department, Faculty of Science, Ain Shams University, 11566 Abbassia, Cairo, Egypt*

The  $\text{Cr}_2\text{O}_3$  doped Oxyfluoroborate Glasses ( $0.55\text{B}_2\text{O}_3\text{-}0.15\text{NaF}\text{-}0.30\text{ZnO}\text{-}x\text{Cr}_2\text{O}_3$ ,  $x=0.0, 0.1, 0.2$  and  $0.3$  mol%) were prepared by the conventional rapid quenching technique. Raman spectroscopy and X-ray scattering were applied to investigate the present glasses. The X-Ray radial distribution function analysis (RDF) showed that the short range order (SRO) of the matrix containing  $\text{ZnO}_4$  units is located at nearly  $2.0\text{\AA}$ , the medium range order (MRO) of the matrix containing the Na-O pairs of the tetrahedral form  $\text{NaO}_4$  is located at  $3.53\text{\AA}$  for the undoped sample but with smaller distances,  $3.45, 3.37, 3.44\text{\AA}$  for the doped  $\text{Cr}_2\text{O}_3$  samples. The next RDF peaks in the MRO revealed the presence of Zn-Zn and Na-Na atomic pairs of octahedral arrangement at average distances of  $4.39$  and  $5.195\text{\AA}$  respectively. The B-O correlations are not observed in the RDF results, while  $\text{ZnO}_4$  units are clearly observed in both previous techniques. A correlation of X-ray radial distribution and Raman spectroscopy is established for the present investigated glasses.

Received July 08, 2014; accepted February 10, 2016)

*Keywords:*  $\text{Cr}_2\text{O}_3$  Oxyfluoroborate Glasses, Octahedral arrangement, Amorphous materials, Radial distribution function, Raman spectroscopy

## 1. Introduction

Zinc borate glasses are interesting materials for optical fibers with a large core diameter and have potential industrial applications between the expensive quartz fibers and high loss polymer fibers. The cations from divalent oxides such as ZnO, when used as modifiers, can produce serious structural effects, this is due to their higher valences which are greater than that of the alkali cations. Zinc ions are surrounded by four oxygen atoms and form a tetrahedral structure whose Zn-O distance is about  $2.0\text{\AA}$  and the neighboring structure of boron atoms transforms from  $\text{BO}_4$  tetrahedral structural units into  $\text{BO}_3$  trigonal structural units with increasing of zinc oxide contents [1, 2, 3].

Vitreous boron trioxide is a transparent glass with refractive index  $\sim 1.48$  in the visible region. The structure of vitreous  $\text{B}_2\text{O}_3$  consists of a random network of boroxol rings and  $\text{BO}_3$  triangles connected by B-O-B linkages. When a modifier oxide is added (alkali oxide, NaO ; e.g.) it causes a transformation of some  $\text{BO}_3$  triangles to  $\text{BO}_4$  tetrahedral units and results in the formation of various cyclic units like diborate, triborate, tetraborate or pentaborate groups with the production of non-bridging oxygen[4-8].

Transition metal ions such as chromium when dissolved in glasses make them colored and have strong influence over the insulating character and optical transmission of these glasses, since  $\text{Cr}_2\text{O}_3$  also participates in the glass network forming with different structural units. Chromium may exist in both  $\text{Cr}^{3+}$  and  $\text{Cr}^{6+}$  states in the glass network.  $\text{Cr}^{3+}$  ion enters in the network as

modifier where  $\text{Cr}^{6+}$  ion enters as network former with  $\text{CrO}_4^{2-}$  structural units[9,10,11].

The objective of this work is; i) to apply X-ray radial distribution function in order to investigate the structure of amorphous  $0.55\text{B}_2\text{O}_3\text{-}0.15\text{NaF}\text{-}0.30\text{ZnO}\text{-}x\text{Cr}_2\text{O}_3$  glasses where  $x=0.0, 0.1, 0.2$  and  $0.3$  respectively in its SRO and MRO ranges ii) to apply Raman spectroscopy in order to reveal the role of doping  $\text{Cr}_2\text{O}_3$  on the structural modification of the studied glasses iii) to correlate the two techniques used in the present investigation with each other iv) to compare the results obtained from the present investigated glasses with other previously similar studied glasses.

## 2. Experimental work

### 2.1. Preparation of samples and measuring its density

Glass disks of 2mm thickness were prepared from chemically pure raw materials. The orthoboric acid ( $\text{H}_3\text{BO}_3$ ) was used to obtain boron oxide  $\text{B}_2\text{O}_3$ . Zinc oxide was introduced in the form of powder of ZnO with purity 99.99%. Sodium Fluoride (NaF) was introduced as such with the ratio 0.15. The ratio of  $\text{Cr}_2\text{O}_3$  was introduced as 0.1, 0.2 and 0.3 mol% respectively.

The chemicals used were accurately weighed by using an electronic balance. The chemicals were then thoroughly mixed and porcelain crucibles containing the batch were placed in electrically heated furnace and kept at  $1100^\circ\text{C}$  for one hour under normal atmospheric conditions. The

crucibles were removed from the furnace and rotated through to produce homogeneous glass.

All the glasses were properly annealed at 400°C temperature in a muffle furnace, then, the muffle furnace was left to cool at a rate of 30°C/hour down to room temperature. Annealing process was done to avoid and minimize the stresses and strains, which may be found in the final glass product. The samples were grounded and highly polished before measurements.

The prepared glasses with molar formula 0.55B<sub>2</sub>O<sub>3</sub>-0.15NaF-0.30ZnO-xCr<sub>2</sub>O<sub>3</sub>(x=0.0, 0.1, 0.2 and 0.3mol%) were used for X-ray radial distribution function (RDF) and Raman spectroscopy studies in this work .

The densities of the prepared glass samples were measured in an indirect method based on Archimedes'

principle using toluene as an immersion liquid, then the density (ρ) of the different Cr<sub>2</sub>O<sub>3</sub>% samples were calculated from the following equation:

$$\rho = \frac{wt_a}{[wt_a - wt_{lq}]} \times \rho_{lq} \text{ gm/cm}^3$$

where wt<sub>a</sub> is the weight of the glass sample in air, wt<sub>lq</sub> is the weight of the glass sample in the immersing liquid and ρ<sub>lq</sub> is the density of the immersing liquid.

The error in the measured density was 0.001gm/cm<sup>3</sup>. Table 1 reports the measured density with the composition of the studied glass elemental percents forming the matrix batches. The values of x versus the matrix density ρ(gm/cm<sup>3</sup>) and O% is depicted in Fig.1.

Table1. Composition and density of the studied glass batches  
Composition 0.55B<sub>2</sub>O<sub>3</sub>-0.15NaF-0.30ZnO-xCr<sub>2</sub>O<sub>3</sub>; x=0.0, 0.1, 0.2 and 0.3mol% respectively

x percent	Cr%	Na%	F%	Zn %	B%	O%	ρ <sub>gm</sub> <sup>3</sup> / <sub>cm</sub>
0.0	0.0	0.049	0.041	0.283	0.175	0.451	2.801
		8					
0.1	0.0015	0.049	0.041	0.283	0.174	0.451	2.829
		7					
0.2	0.0032	0.049	0.041	0.282	0.174	0.450	2.797
		6					
0.3	0.0044	0.049	0.041	0.307	0.174	0.456	2.851
		3					

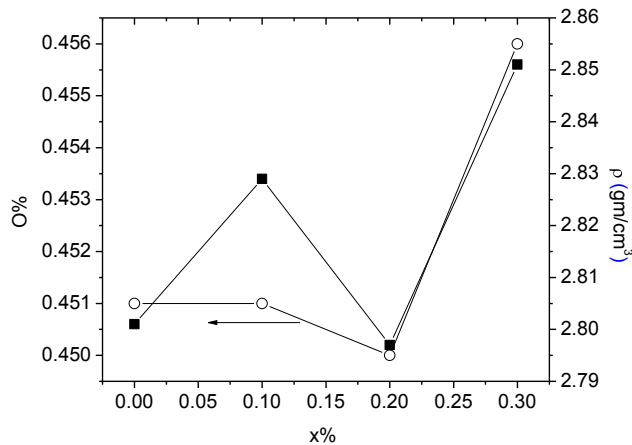


Fig. 1. The Cr<sub>2</sub>O<sub>3</sub> added mol% versus the density and O% of the studies B<sub>2</sub>O<sub>3</sub>-ZnO- NaF glasses

Dispersive Raman Spectrometer (BRUKER-SENTERRA, Germany) equipped with an integral microscope (Olympus) is used to record the Raman spectra of all the prepared glass samples in the wave number range 100-1800cm<sup>-1</sup>.

### 2.2 XRD apparatus setup

The present data were collected by using Philips (X'pert MPD) diffractometer using the Bragg-Brentano para-focusing technique. Highly monochromated Cu-radiation (wavelength λ=1.541Å) was used. The step scan

mode was applied in the 2θ-range (4-157.4612°). The step size (Δ2θ=0.04°) and the counting time was 10 seconds for each reading. The corresponding accessible maximum scattering vector magnitude, K, was 8.0Å<sup>-1</sup>(K=4πsinθ/λ). The air scattering was avoided by a suitable applied arrangement of XRD system. The receiving and divergence slits were properly chosen in both small and large 2θ-ranges, in order to improve the qualities of data collected.

### 2.3 The relation between S (K) and RDF (r)

The scattered intensity in the K-space, I( K ), was corrected for the polarization and absorption factors, then scaled and normalized to get on the self scattered intensity and the structure factor S(K) in the reciprocal space[12-15]. The total structure factor of a glass[12] is given by :

$$S(K) = \{ I(K) - [\Re f^2 \phi) - \Re f \phi^2] \} / \Re f \phi^2 \quad (1)$$

Where the term [ℑf<sup>2</sup>ϕ)-ℑfϕ<sup>2</sup>] is known as the Laue diffraction and is more significant at small angle 2θ of X-ray scattering. The RDF is given by: [12]

$$RDF = 4\pi r^2 \rho(r) = 2r/\pi \int K[S(K)-1] \exp(-\alpha^2 K^2) \sin(Kr) dK \quad (2)$$

Where ρ(r) is the sample atomic density as a function of the radial distance r, α is the disordering parameter of value~0.1Å which is mainly used to reduce the effect of spurious details in the high K-range in the measured data.

### 3. Results and discussion

#### 3.1. Raman measurements

The Raman spectrum of the first sample ( $0.55\text{B}_2\text{O}_3\text{-}0.15\text{NaF}\text{-}0.30\text{ZnO}$ ) which has no  $\text{Cr}_2\text{O}_3$  contents is shown in Fig.2-0. It can be seen from the figure that there is a main prominent peak at  $1295.22\text{cm}^{-1}$  of larger intensity and of higher broadening and dominates for all the studied samples. This main peak is belonging to pyroborate units ( $\text{B}_2\text{O}_5^{4-}$ ) of larger non-bridging oxygen (NBO) bond compared with the other B-O bonds connections. Another broad weak peak is seen at  $1486.88\text{cm}^{-1}$  which was found to be due to  $\text{B-O}^-$  vibrations of varied bonds [Sudhakar et al., [1]]. Three other peaks of ( $\text{B}_2\text{O}_5^{4-}$  pyroborate units), are revealed at lower wave numbers,  $801.8\text{cm}^{-1}$  and  $713.11\text{cm}^{-1}$  which are due to the chain type of (metaborate units  $\text{B}_3\text{O}_6^{3-}$ ) also the peak at  $501.84\text{cm}^{-1}$  is due to the (diborate units  $\text{B}_4\text{O}_7^{2-}$ ). Another set of sharper and weaker Raman peaks are also present at lower wave numbers which may be due to B-O dangling bonded units [1].

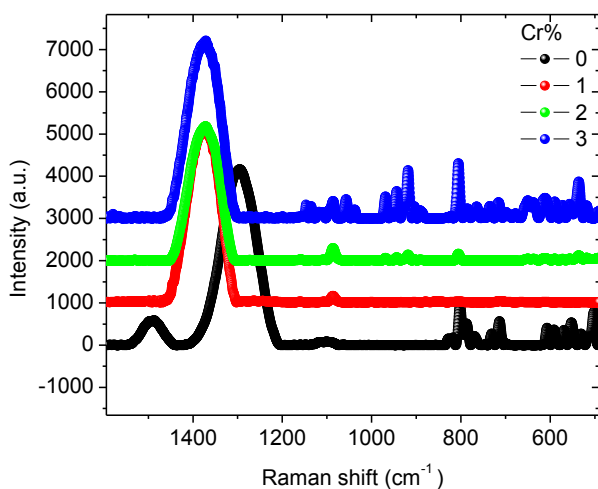


Fig.2 The Raman shift in  $\text{cm}^{-1}$  versus the Raman intensity vibrations of the studied glasses ( $\text{B}_2\text{O}_3\text{-ZnO-NaF-Cr}_2\text{O}_3$ ) with  $\text{Cr}_2\text{O}_3$  percent 0.0, 0.1, 0.2 and 0.3 respectively.

The Raman Spectrum of the second sample ( $0.55\text{B}_2\text{O}_3\text{-}0.15\text{NaF}\text{-}0.30\text{ZnO}\text{-}0.1\text{Cr}_2\text{O}_3$ ) which has 0.1mol%  $\text{Cr}_2\text{O}_3$  is shown in (Fig.2-1). As shown from this figure, the main prominent peak is the only presented peak but instead of being located at  $1295.22\text{cm}^{-1}$  it is shifted to a longer wave number at  $1371\text{cm}^{-1}$  moreover there is an increase in its peak sharpening which indicates that there is an increase in the atomic ordering of the glass matrix, i.e, more matrix packing and increase in its density. Moreover, all the previous Raman peaks (or details) shown in Fig.2-0 others than the main peak disappeared. The high packing of the atoms and accordingly the high density will lead to, the stabilization of the pyroborate units( $\text{B}_2\text{O}_5^{4-}$ ). It can be also suggested that the linkages Zn-O-Cr and B-O-Cr will be formed to fill the matrix interstices as a structural change in the matrix due to the introduction of  $\text{Cr}_2\text{O}_3$ . The enhanced samples density and high packing of its atoms is supported

by Fig.1(and also table1), and meanwhile reveals the percent decrease of oxygen voids inside the studied glass. Accordingly, the matrix interstices will be filled by the Cr atoms/ions in the form of previous linkages with the small added percents of  $\text{Cr}_2\text{O}_3$ (0.0-0.1mol%). In contradiction, with the high added percents of  $\text{Cr}_2\text{O}_3$ (0.2-0.3mol%) the matrix disorder increases and both of density and packing of atoms of the glass going to decrease due to the formation of Cr-O-Cr linkages instead of Zn-O-Cr and B-O-Cr ones. This means that Cr(atoms/ions) could replace each of Zn and B causing an increased disorder of the studied glass and also activate a conversion of  $\text{BO}_3$  units into  $\text{BO}_4$  motifs.[1].

Fig.2-2 shows the Raman Spectrum of the third sample ( $0.55\text{B}_2\text{O}_3\text{-}0.15\text{NaF}\text{-}0.30\text{ZnO}\text{-}0.2\text{Cr}_2\text{O}_3$ ), as it can be seen the main principal Raman peak located at  $1371\text{cm}^{-1}$  is still observed, but with a decrease in its intensity, other minor peaks are also present, located at 1086, 805, and  $535\text{cm}^{-1}$ , they have very weak intensities and also weak oscillations. These very weak peaks are due to; diborate units( $\text{B}_4\text{O}_7^{2-}$ ), Boroxol ring( $\text{B}_3\text{O}_6$ ) and isolated diborate units( $\text{B}_4\text{O}_7^{2-}$ ) respectively [1]. This means that the small evolved Raman peaks are grown on the expense of pyroborate groups( $\text{B}_2\text{O}_5^{4-}$ ) [Sudhakar et al.]. Fig.2-3 shows the Raman spectrum of the fourth sample ( $0.55\text{B}_2\text{O}_3\text{-}0.15\text{NaF}\text{-}0.30\text{ZnO}\text{-}0.3\text{Cr}_2\text{O}_3$ ), as it can be seen from the figure, there is a main prominent peak which is more or less similar to the main peak of the undoped sample which was shown in Fig.2-0. Beside this main peak, there are also three other minor peaks which are located at 918, 805, and  $535\text{cm}^{-1}$  respectively. The new evolved peaks are of larger intensity and the peak due to Boroxol ring was highly grown at ( $805\text{cm}^{-1}$ ). One can observe that the other matrix pairs of Zn-O are evidenced at  $282\text{cm}^{-1}$  in the form of  $\text{ZnO}_4$  units having weak intensity. The other pairs such as Na-O or F-... and Cr-O correlations have no, observed Raman vibrations.

#### 3.2. X-ray RDF study

The structure factors of the investigated samples are shown in Fig.3. The limited K-value of the reciprocal space ( $8.0\text{\AA}^{-1}$ ), reduced the amount of data resolution in both K and r-spaces respectively. The undoped sample, i.e, the sample which is totally free of any  $\text{Cr}_2\text{O}_3$ , has a similar S(K) to the third sample (0.2mol% of  $\text{Cr}_2\text{O}_3$ ) but with the first S(K) peak shifted to larger K values. The 0.1mol%  $\text{Cr}_2\text{O}_3$  second sample showed approximately S(K) values similar to that of the (0.3mol%  $\text{Cr}_2\text{O}_3$ ) fourth sample. Moreover, the first peak of the second sample is more broader than that of the fourth one. The MRO (medium range order) of the fourth sample is highly ordered compared to that of the first undoped sample. The first peak of S(K) for undoped sample is revealed at  $\sim 2.2\text{\AA}^{-1}$  but suffers a larger K- peak shift in the first sample when adding 0.1mol%  $\text{Cr}_2\text{O}_3$  to be at  $2.269\text{\AA}^{-1}$ . The second and successive peaks of S(K) for all the samples are of composite structure; with more than one pre- and post shoulders.

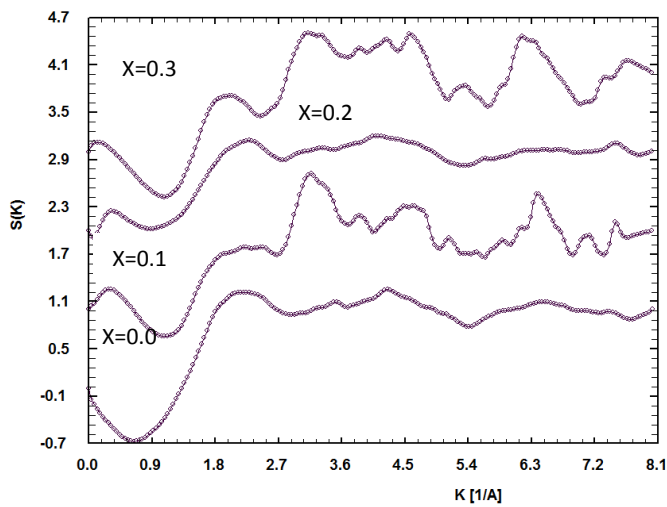


Fig. 3. Total Structure Factor of Amorphous  $B_2O_3$ -ZnO-NaF- $Cr_2O_3$ ; with  $Cr_2O_3$  Percent 0.0, 0.1, 0.2, and 0.3 mol% respectively from bottom to top

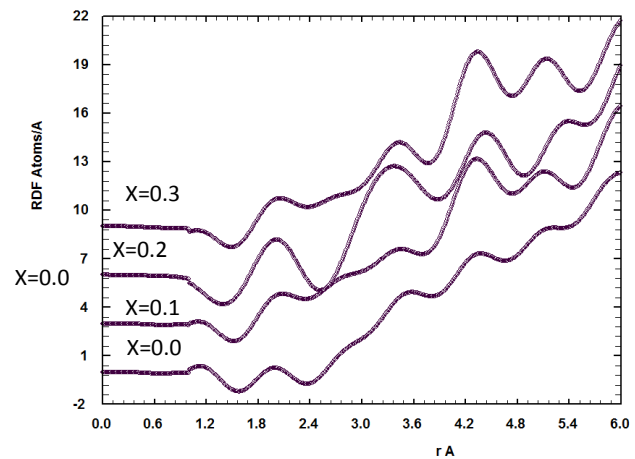


Fig.4 RDF Versus  $r$  for Amorphous  $B_2O_3$ -ZnO-NaF- $Cr_2O_3$ ; with  $Cr_2O_3$  Percents 0.0, 0.1, 0.2, and 0.3 mol% respectively from Bottom to Top

Fig.4 depicts the RDF (Radial Distribution Function) versus  $r$  for the studied samples. The first observed peak for the undoped sample was centered at  $2.0\text{\AA}$  ( $r_1 \pm 0.04\text{\AA}$ ) and had a coordination number of nearly 3.459. This peak was revealed also at more or less the same position in the third sample (0.2 mol%  $Cr_2O_3$ ), but with increase in the coordination number (3.85). The second (0.1 mol%  $Cr_2O_3$ ) and fourth samples (0.3 mol%  $Cr_2O_3$ ) have their first peak located at  $2.045\text{\AA}$  with coordination number about 3.6. This peak is due to Zn-O correlations of tetrahedral units  $ZnO_4$ . The second RDF peak was found at  $3.53\text{\AA}$  for first undoped sample and it was shortened to be at  $3.45$ ,  $3.37$ ,  $3.43\text{\AA}$  for the second, third and fourth samples respectively with the addition of their corresponding  $Cr_2O_3$ % to the given matrix. The RDF second peak is due to the Na-O pairs of an average coordination number 4.0 which explains the formation of  $NaO_4$  tetrahedra. The shift of  $r_2$  to the smaller distances with the doping of  $Cr_2O_3$  means the increased order of the matrix in the vicinity of SRO. One can observe generally the increased order of MRO of the amorphous studied systems with the percentage increase in the added  $Cr_2O_3$ %. The third RDF peak which represents the third coordination shell,  $r_3$ , appeared at  $4.46\text{\AA}$  for the first and third samples and shifted to  $4.33\text{\AA}$  for the second and fourth samples. This third shell is attributable to Zn-Zn correlations which represents the octahedral arrangement. The next fourth RDF peak which represents the fourth coordination shell,  $r_4$ , was observed at  $5.17\text{\AA}$  and highly stretched to be at  $5.358\text{\AA}$  for the third sample and it was centered at the same distance,  $5.169\text{\AA}$ , for the second and fourth samples. This fourth coordination shell is due to Na-Na correlated pairs of also octahedral arrangement but, with larger disorder compared to Zn-Zn ordered pairs. For all the studied samples of the structural formula ( $0.55B_2O_3$ - $0.15NaF$ - $0.30ZnO$ - $xCr_2O_3$ , ( $x=0.0, 0.1, 0.2$  and  $0.3\text{mol\%}$ )) a small shoulder can be observed at  $2.8\text{\AA}$  which may be due to Zn-Zn correlations of nearly coordination number 1.0 inside SRO.

The B-O linked pairs of the different forms;  $BO_3$  and/or  $BO_4$ , are not revealed in the collected RDF information, this is probably due to the weak scattering of the X-ray by the two light atoms; B and O. Similarly the atomic or ionic fluorine linkages are not revealed in the RDF results. By comparing the information obtained from RDF with those obtained from Raman spectroscopy, one can find that only  $ZnO_4$  and different correlated borates of oxygen environments were observed by Raman such as ( di, tri, tetra, penta and pyroborates, ...) and also NBO are created by introducing  $Cr_2O_3$  in the matrix. As a consequence, the applied X-ray RDF analysis and Raman measurements are complementary techniques; in exploring the B-O different linkages via the Raman vibrations and Zn-O correlations observed by the two applied techniques. Also, the small percents introduced of  $Cr_2O_3$  (matrix former) enhanced the matrix order and its packed density, while the increased percents of  $Cr_2O_3$  (matrix modifier) distorts the matrix order (increasing matrix disorder) which was evidenced by the applied techniques.

Our obtained findings are supported by many other workers and a good comparison is established with the results reported by Sudhakar et al. [1]. They are treated more similar glasses with those of us except of adding small percents of  $Cr_2O_3$  (0.0-0.1 mol%).

#### 4. Conclusion

The results showed that; by introducing 0.1 mol%  $Cr_2O_3$  in the oxyfluoroborate matrix ( $0.55B_2O_3$ - $0.15NaF$ - $0.30ZnO$ - $0.1Cr_2O_3$ ) a high medium range ordering (MRO) was observed. This ordering was mainly due to the formation of Zn-O-Cr and B-O-Cr linkages which can fill the matrix interstices and lead to an increase in the matrix packing and accordingly an increase in its density. By increasing  $Cr_2O_3$  content by 0.2 mol% an enhanced

ordering in both short range ordering (SRO) and medium range ordering (MRO). On the other hand the 0.3mol% of  $\text{Cr}_2\text{O}_3$  sample has a larger MRO ordering compared to its (SRO) ordering. One can suggest from the previous analysis that, by introducing different percentage of the  $\text{Cr}_2\text{O}_3$  in the studied samples, the smaller percentages of  $\text{Cr}_2\text{O}_3$  will act as a matrix former, with the formation of ( $\text{CrO}_4^{2-}$  units). On the other hand, the higher  $\text{Cr}_2\text{O}_3$ mol% will act as a matrix modifier creating Cr-O-Cr linkages and moreover transforming  $\text{BO}_3$  units into  $\text{BO}_4$  which cause more disordered matrix. Moreover, the (RDF) and the Raman results confirmed both the presence of Zn-O correlations at nearly  $2.0\text{\AA}$ , which indicate the presence of the tetrahedral arrangements of the  $\text{ZnO}_4$ . Raman study of the given glasses clearly evidenced the presence of the different borate systems as( di, tri, tetra, penta and pyroborates, ...) and also NBO were created. The Na-O pairs are observed in MRO as  $\text{NaO}_4$  motifs at a distance of  $3.43\text{-}3.37\text{\AA}$  with the introduction of  $\text{Cr}_2\text{O}_3$  and also Na-Na and Zn-Zn are revealed as octahedral forms at ( $5.17\text{-}5.36\text{\AA}$ ), ( $4.33\text{-}4.46\text{\AA}$ ) respectively. It was found also that Cr-ions play the former role as well as the modifier one in the studied glass ( $\text{Cr}^{6+}$  and  $\text{Cr}^{3+}$  respectively). A good support of the present work was reported by Sudhakar et al.[1] for  $20\text{CaF}_2\text{-}20\text{ZnO}\text{-}(60\text{-}x)\text{B}_2\text{O}_3\text{-}x\text{Cr}_2\text{O}_3$  ( $0 \leq x \leq 0.1$ mol%) glass samples which has nearer composition to the present studied composition but with small added percents of  $\text{Cr}_2\text{O}_3$ .

## References

- [1] B. K. Sudhakar, N. R. K. Chand, H. N. L. Prasanna, G. Srinivasa Rao, K. Venkateswara Rao, Vivek Dhand, *J. of Non-Cryst. Solids*, **356**, 221 (2010).
- [2] A. Ivankov, J. Seekamp, W. Bauhofer, *Mater. Lett.* **49**, 209 (2001).
- [3] S. Rada, P. Pascuta, L. Rus, M. Rada, E. Culea *J. of Non-Crystalline Solids*, **30**, 358 (2012).
- [4] P. Pascuta, R. Langu, I. Ardelean, *J. Mater, Sci. Mater. Electron*, **21**, 548 (2010).
- [5] P. Pascuta, I. Pop, S. Rada, E. Culea, *J. Mater, Sci. Mater. Electron*, **19**, 424(2008).
- [6] Byung-Sook Kim, Eun-sub Lim, Jeong-Joo Kim, *J. Mater. Sci.* **42**, 4260(2007).
- [7] E. Mansour, *Physica* **B362**, 88 (2005).
- [8] Longfei Zhou, H. Lin, W. Chen and I. Luo, *J. Phys. Chem. Solids* **69**, 2499 (2008).
- [9] L. Stoch, M. Sroda, *J. Mol. Struc.* **77**, 511-512(1999).
- [10] G. Srinivasa Rao, N. Veeraiak, *Eur. Phys. J. appl.* **16**, 11 (2001).
- [11] G. Srinivasa, N. Veeraiak, *J. Phys. Chem. Solids* **36**, 705 (2002).
- [12] A. Abou Shama, A. Abd-Allah, G. MA. Youssef, *J. of Optoelectron. Adv. Mater.* **16**(5-6), 677 (2014).
- [13] J. Krogh-Moe, *Acta Cryst.* **9**, 951(1956).
- [14] N. Norman, *Acta Cryst.* **10**, 370(1957).
- [15] A. C. Wright, C. A. Yarker, P. A. V. Johnson, R. N. Sinclair, *J. of Non-Cryst. Solids* **104**, 323(1988).

\*Corresponding author: aboushamaali@yahoo.com